JOURNAL OF FOREST SCIENCE

Volume 51, No. 2 **February 2005**

CONTENTS

Zawadzki J., Cieszewski Ch. J., Zasada M.: Semivariogram analysis of Landsat 5 TM textural data for loblolly pine forests 47

Podrázský V. V., Remeš J.: Effect of forest tree species on the humus form state at lower altitudes 60

Tokár E., Krekulová E.: Structure, quality, production, LAI and dendrochronology of 100 years old Austrian pine (*Pinus nigra* ARNOLD*)* stand 67

Hrázský J., Král P.: Assessing the bending strength and modulus of elasticity in bending of exterior foiled plywoods in relation to their construction 77

OBSAH

Zawadzki J., Cieszewski Ch. J., Zasada M.: Semivariogramová analýza textury dat z Landsatu TM 5 u porostů borovice kadidlové (*Pinus taeda* L.) 47

Podrázský V. V., Remeš J.: Vliv lesních dřevin na stav humusových forem v nižších polohách 60

Tokár E., Krekulová E.: Vývoj štruktúry, kvality, produkcie a dendrochronológie 100-ročného rovnorodého porastu borovice čiernej (*Pinus nigra* ARNOLD) 67

Hrázský J., Král P.: Posouzení pevnosti v ohybu a modulu pružnosti v ohybu vodovzdorných fóliovaných překližek v závislosti na jejich konstrukci 77

INSTITUTE OF AGRICULTURAL AND FOOD INFORMATION

Slezská 7, 120 56 Prague 2, Czech Republic

Tel.: + 420 227 010 111, Fax: + 420 227 010 116, E-mail: redakce@uzpi.cz

In this institute scientific journals dealing with the problems of agriculture and related sciences are published on behalf of the Czech Academy of Agricultural Sciences. The periodicals are published in English with abstracts in Czech.

Journal	Number of issues per year	Yearly subscription in USD
Plant, Soil and Environment	12	285
Czech Journal of Animal Science (Živočišná výroba)	12	285
Agricultural Economics (Zemědělská ekonomika)	12	285
Journal of Forest Science	12	285
Veterinární medicína (Veterinary Medicine – Czech)	12	285
Czech Journal of Food Sciences	6	129
Plant Protection Science	4	85
Czech Journal of Genetics and Plant Breeding	4	85
Horticultural Science (Zahradnictví)	4	85
Research in Agricultural Engineering	4	85

Subscription to these journals be sent to the above-mentioned address.

Semivariogram analysis of Landsat 5 TM textural data for loblolly pine forests

J. Zawadzki[1], Ch. J. Cieszewski[2], M. Zasada[3]

[1]*Environmental Engineering Department, Warsaw University of Technology, Warsaw, Poland*
[2]*Warnell Scholl of Forest Resources, University of Georgia, Athens, USA*
[3]*Department of Forest Productivity, Faculty of Forestry, Warsaw Agricultural University, Warsaw, Poland*

ABSTRACT: The objective of this study was to evaluate the applicability of Landsat 5 TM images for analysing the textural information on pine forest stands in western Georgia, United States. Analysing spatial correlations between pixels measured by semivariances and cross-semivariances (cross-correlation between two radiometric bands) calculated from transects of Landsat TM images, we explored differences between semivariances associated with images of stands of various ages, origins (natural vs. planted) and species (loblolly pine – *Pinus taeda* L. – versus longleaf pine – *Pinus palustris* Mill.). We analysed both ground measurements and the satellite images using the visible, the near infrared, and the middle-infrared bands. We also analysed semivariances and cross-semivariances calculated from the Normalized Difference Vegetation Index and the Ratio Vegetation Index. The results showed that in spite of the relatively low Landsat TM spatial resolution (30m) the semivariograms and cross-semivariograms provided potentially useful information about the above-mentioned classes. The semivariances and cross-semivariances calculated from Landsat TM images of loblolly pine stands depend both on the age and the stand origin. In particular, large differences exist in semivariance and cross-semivariance sills. Significant differences also exist between semivariances calculated from stands of loblolly and longleaf pine.

Keywords: semivariance; textural classification; remote sensing; loblolly pine; Landsat TM

Field measurements are the most exact way to collect detailed information about forest properties, but such data collection is expensive and time consuming. In most cases remote sensing is a less expensive supplement to ground measurements and is frequently used in forest inventories due to its cost efficiency and timely capabilities over large areas, and it may be used for assessment of various forest and ecosystem information (Campbell l994; De Fries, Townshend 1994; Vogelmann et al. 1998). One of the main disadvantages of single-sourced remote sensing measurements is that data are usually collected at a single spatial resolution. Different airborne techniques can collect data at a variety of spatial resolutions, but most of them are still very expensive. High-resolution remote sensing data are more costly than low-resolution data to both purchase and process.

The most commonly used methods for image classification of remotely sensed images are applied on a pixel-by-pixel basis without considering potentially useful spatial information among neighbouring pixels. Semivariances quantify certain spatial information and have been proven very useful in the analysis of various spatial data (Carr 1966; Woodcock, Strahler 1988a,b; Curran 1988). Up to now, the semivariances have been successfully used in forestry applications, but only in the case of expensive high-resolution data (St-Onge, Cavayas 1995; Treitz, Howarth 2000). Song and Woodcock (2002) demonstrated the potential of multi-resolution remote sensors for research of forest succession.

If the semivariance has a classic form, it is a very efficient tool in remotely sensed image analysis. For example, it can be used for estimating the necessary spatial resolution because its range determines the distance above which ground resolution elements are not related (Curran 1988). Ramstein and Raffy (1989) stated that land cover classes could be well differentiated by the semivariance range (assuming an exponential semivariance model). Many present studies (St-Onge, Cavayas 1995; Wallace et al. 2000) show that range and sill should be taken together for this purpose. However, it is not very clear if spatial pattern information produced by the semivariances calculated from low-resolution remote sensing images could improve a broad-scale forest classification (Strahler et al. 1986). There are also some important difficulties in the application of semivariance for forest classification. Very often semivariances of forested areas are much more complicated than the "classic" form described in the literature, and can show periodic and aspatial variations. The first type of semivariance occurs in studies of repetitive patterns while the second one occurs when studying random patterns. These kinds of semivariances have been reported and described e.g. by Curran (1988), and they are much more difficult to model and interpret. The usefulness of "non-classic" types of semivariances for classification is usually considerably less due to severe difficulties in estimation of their parameters. In addition, because of the large file sizes of remotely sensed images, accurate semivariance modelling is computationally unreasonable. Instead of the accurate modelling of semivariances most authors propose to calculate a set of texture measures of spatial variability (TMSV) or semivariances for the first consecutive lags (semivariance textural classifier algorithm, STC) within a moving window based on the semivariance value (Chica-Olmo, Abarca-Hernandez 2000; Miranda et al. 1992, 1996). Recently, several other parameters of semivariance were also analysed for classification using parameters that do not require modelling, e.g. semivariances at consecutive lags, ratios of semivariances for consecutive pairs of lags, the slope of the semivariance for consecutive pairs of lags, mean semivariance and different measures of semivariance shape (Herzfeld, Higginson 1996; Jakomulska, Clarke 2001).

The results of applications of low-resolution remote sensors for observations of forested areas are rather scarce. Woodcock et al. (1988a,b) calculated semivariances from remote images of forested areas using one visible (red) band of the Thematic Mapper sensor at a 30-meter spatial resolution. Miranda et al. (1992, 1996) used relatively inexpensive microwave images to classify Brazilian rainforest. Using both high and low resolution remote sensing images of conifer canopy structure, Cohen et al. (1990) concluded that the range of semivariances calculated using Landsat TM data was not useful for estimating tree crown sizes. The authors also indicated that sills of these semivariances were very similar in magnitude. However, calculations were limited only to the visible portion of the image spectrum and did not combine multiple-band textural information.

The Landsat TM satellite is appropriate for mapping and investigating broad vegetative types. It uses three bands in the visible portion of the spectrum, three bands in the reflective-infrared portion of the spectrum and one band in the thermal portion of the spectrum. The spatial resolution of the TM sensor of the Landsat satellite is 30 metres for the visible bands and 120 metres for the thermal band. Landsat TM data are relatively inexpensive; satellite images of areas located in the USA can be purchased from the EROS Data Center for approximately $500–600 per each 185 × 185 km scene (prices as for May 2003). Classification methods based on spectral information from Landsat TM images are appropriate for discriminating between classes with sufficiently different spectral characteristics. For example, it is

Table 1. Some forest parameters for the studied stands of loblolly pine and longleaf pine

Stand	Number (N)	Area (ha)			Stems per ha			Site index (base 25)			Basal area (m²/ha)		
		mean	min	max	mean	min	max	mean	min	max	mean	min	max
Loblolly planted young	47	86.2	33.4	235.8	1,766	1,216	2,506	56	48	65	10.07	4.59	18.37
Loblolly planted medium	35	80.2	57.8	207.4	1,406	561	1,730	59	48	65	21.67	11.50	26.87
Loblolly natural young	10	4.5	0.2	10.5	1,103	247	1,977	56	53	59	×	×	×
Loblolly natural medium	36	8.1	0.4	68.1	801	247	1,545	62	56	63	8.04	5.74	17.22
Loblolly natural old	34	10.2	6.6	13.7	504	247	1,483	58	55	63	14.9	6.89	22.96
Longleaf planted medium	5	25.1	0.7	78.3	487	200	500	55	45	56	4.65	4.59	5.74
Longleaf natural old	5	26.6	6.1	31	355	275	450	52	40	56	8.27	3.67	14.24

relatively easy to discriminate between water, fields, and hardwood and coniferous forests (Bauer et al. 1994; Evans 1994). A more difficult situation occurs when spectral characteristics of studied areas are very similar (e.g. for various coniferous stands, Brockhaus, Khorram 1992). In this case texture information can be essential.

The objective of this study was to evaluate the applicability of relatively inexpensive, low-resolution Landsat 5 TM images for analysing the textural information of the images of loblolly pine forests (*Pinus taeda* L.) in western Georgia, USA, using geostatistical methods. Loblolly pine is the most important timber tree in the southeastern USA. Occupying approximately 12 million hectares (both natural stands and plantations), the species has accounted for nearly 60% of all seedlings planted in the USA (Sheffield, Knights 1982). We analysed different ages and origins of loblolly pine stands using semivariances and cross-semivariances. To check if semivariances can discriminate between different species, we compared semivariances for loblolly pine with those of longleaf pine (*Pinus palustris* Mill.).

MATERIAL AND METHODS

In this study remote sensing images were related to vegetation data through the use of ground-validation data collected in the field. The study area was located in the western part of the state of Georgia, USA. The ground reference forest data was covered by the Landsat TM scene, path 019/row 37, collected in November 1997. The ground data collected for each reference site contained stand level information including stand-polygon GIS/GPS coordinates, vegetation type (e.g. species) as well as quantitative data (e.g. age, diameter at breast height, basal area, and density).

To calculate reliable semivariances we limited our subject data to large loblolly pine stands described in Table 1. In order to compare the loblolly pine stand textural characteristics with another species we also used data from longleaf pine stands. We divided all studied stands into three age classes: young (6–15 years old), medium (16 to 30 years old) and old (older than 30 years). We differentiated also between planted and natural stands. We used data collected for 162 stands of loblolly pine (82 planted and 80 natural). No ground data for old planted stands of loblolly pine was available. In order to show the effect of the pine species on semivariance we also used data collected from medium-age planted longleaf pine stands (16–30 years old) and from old natural longleaf pine stands (older than 30 years). Some characteristics of the studied classes of forest stands are given in Table 1.

In this study we used digital numbers (DN) from the RED band (red, 0.63–0.69 μm), the NIR band (reflective-infrared, 0.76–0.90 μm) and the MIR band (mid-infrared 1.55–1.75 μm). The RED band is sensitive enough to discriminate between plant species. The NIR band is especially sensitive to the amount of vegetation biomass present in a scene. The MIR band is sensitive to the amount of water in plants (ERDAS Field Guide 1990). Together with the spectral characteristics of the images we also studied the geostatistical characteristics of the Normalized Difference Vegetation Index (NDVI) introduced by Rouse (Rouse et al. 1973; Nemani et al. 1993) as well as the Ratio Vegetation Index (RVI) proposed by Jordan (Jordan 1969; De Jong 1994; Brown et al. 2000). The NDVI index has been found to be a sensitive indicator of the presence and condition of green vegetation (Tucker et al. 1986) whereas the Ratio Vegetation Index is sensitive to the existence of forest underbrush (Brown et al. 2000).

Geostatistics comprises many methods for evaluating the autocorrelation that commonly exists in spatial data. The central tool of geostatistics is semivariance that is a measure of spatial continuity. The graphical expression of the semivariance is the semivariogram. The application of the semivariance requires that the data meet the intrinsic hypothesis for a regionalised variable (Journel, Huibregts 1978). This hypothesis requires that the expected value of differences in data is zero for all vectors **h** separating any two points in the region of interest, and that the semivariance in the data is a function only of the vector **h** between samples.

Semivariance (γ) is half the expected squared difference between values of data at a distance of separation or lag, **h**, a vector in both distance and direction. The experimental semivariance $\gamma(\mathbf{h})$ is calculated as:

$$\gamma(\mathbf{h}) = \frac{1}{2N(\mathbf{h})} \sum_{i=1}^{N(\mathbf{h})} [Z(x_i) - Z(x_i + \mathbf{h})]^2 \qquad (1)$$

where: **h** – lag (in pixels) over which γ (semivariance) is measured,

N – the number of observations used in the estimate of $\gamma(\mathbf{h})$,

Z – the value of the variable of interest at spatial position $\boldsymbol{x}_i$.

The value $Z(\boldsymbol{x}_i + \mathbf{h})$ is the variable value at lag **h** from **x**.

Semivariances are roughly summarised by three characteristics:

Table 2. Minimum, maximum, mean, and standard deviation of DN values calculated from Landsat 5 TM images of investigated loblolly and longleaf pine stands

		Loblolly pine					Longleaf pine	
		planted		natural			planted	natural
		young	medium	young	medium	old	medium	old
RED	minimum	11.00	10.00	13.00	11.00	12.00	13.00	12.00
	maximum	52.00	43.00	31.00	41.00	37.00	39.00	53.00
	mean	18.74	15.19	19.91	16.06	16.35	20.71	21.49
	std. dev.	3.28	2.20	3.95	2.95	2.41	3.00	5.31
NIR	minimum	14.00	12.00	21.00	22.00	11.00	24.00	55.00
	maximum	63.00	58.00	47.00	53.00	55.00	54.00	0.53
	mean	38.84	35.96	34.56	37.88	32.44	36.70	34.75
	std. dev.	4.48	4.64	6.48	4.38	3.99	2.89	5.44
MIR	minimum	14.00	5.00	20.00	14.00	2.00	24.00	10.00
	maximum	108.00	103.00	86.00	93.00	87.00	107.00	118.00
	mean	42.82	27.63	47.38	30.15	34.19	51.08	52.08
	std. dev.	11.81	7.81	14.93	9.79	7.71	9.14	18.71
NDVI	minimum	–0.15	–0.20	0.00	–0.03	–0.42	0.075	–0.01
	maximum	0.59	0.63	0.52	0.57	0.51	0.053	0.52
	mean	0.30	0.40	0.24	0.40	0.33	0.28	0.24
	std. dev.	0.14	0.08	0.13	0.10	0.07	0.07	0.10
RVI (NIR/RED)	minimum	1.00	0.28	1.43	1.00	1.00	1.6	0.83
	maximum	3.65	3.44	3.27	3.19	3.21	3.25	3.34
	mean	2.26	1.80	2.41	1.85	2.08	2.46	2.37
	std. dev.	0.33	0.28	0.36	0.32	0.26	0.22	0.39

- sill – the plateau that the semivariance reaches. The sill is the amount of variation explained by the spatial structure;
- range of the influence (correlation). The distance at which the semivariance reaches the sill;
- nugget effect – the vertical discontinuity at the origin. The nugget effect is a combination of sampling error and short-scale variations that occur at a scale smaller than the closest sample spacing. The sum of the nugget effect and sill is equal to the variance of the sample.

Remotely sensed images can also be used in semivariance calculations. In this study semivariances were calculated for each stand separately using the digital numbers (DN) or vegetation indices from the remotely sensed images as data values $Z(x_i)$. We calculated the

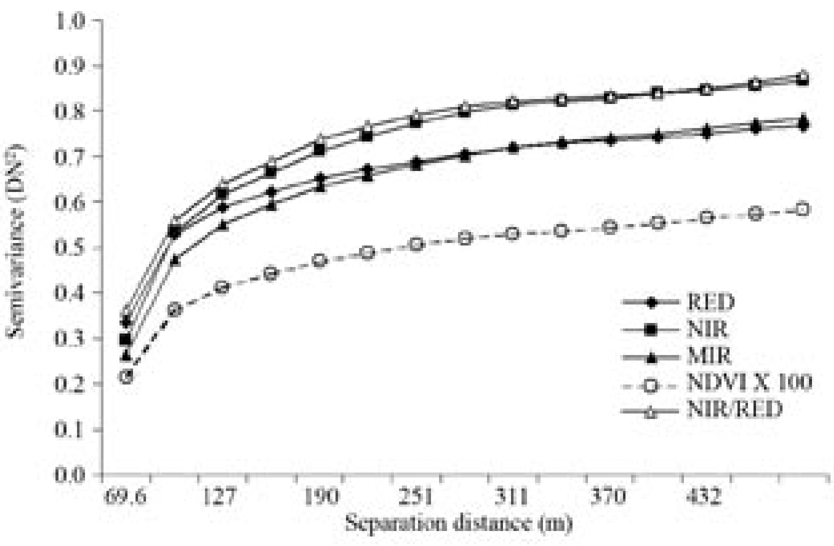

Fig. 1. Isotropic semivariances calculated from Landsat 5 TM images of a loblolly pine stand planted in 1988

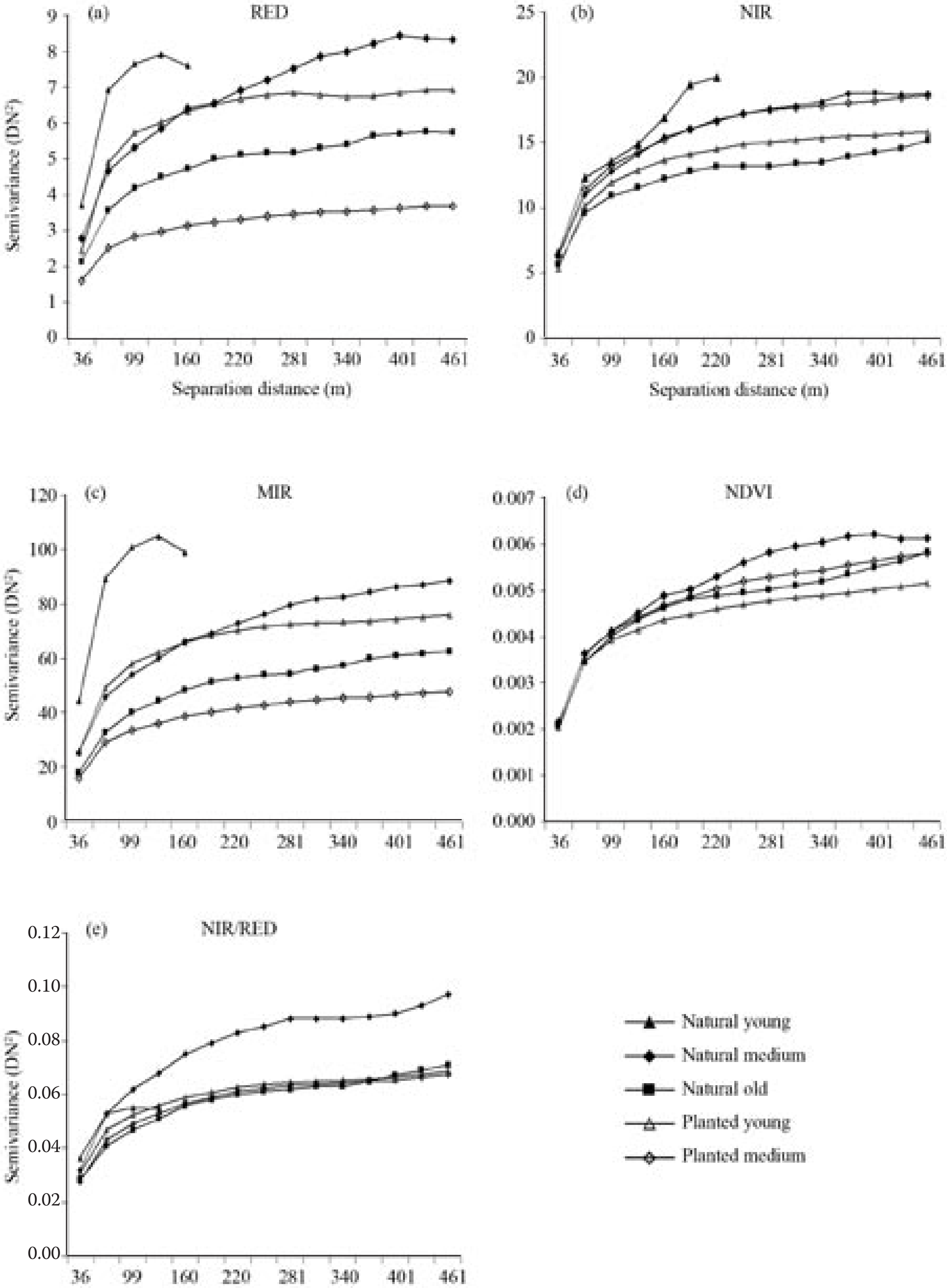

Fig. 2. Isotropic semivariances for different types of loblolly pine stands, calculated from Landsat 5 TM images using: (a) RED channel, (b) NIR channel, (c) MIR channel, (d) NDVI, and (e) RVI (NIR/RED)

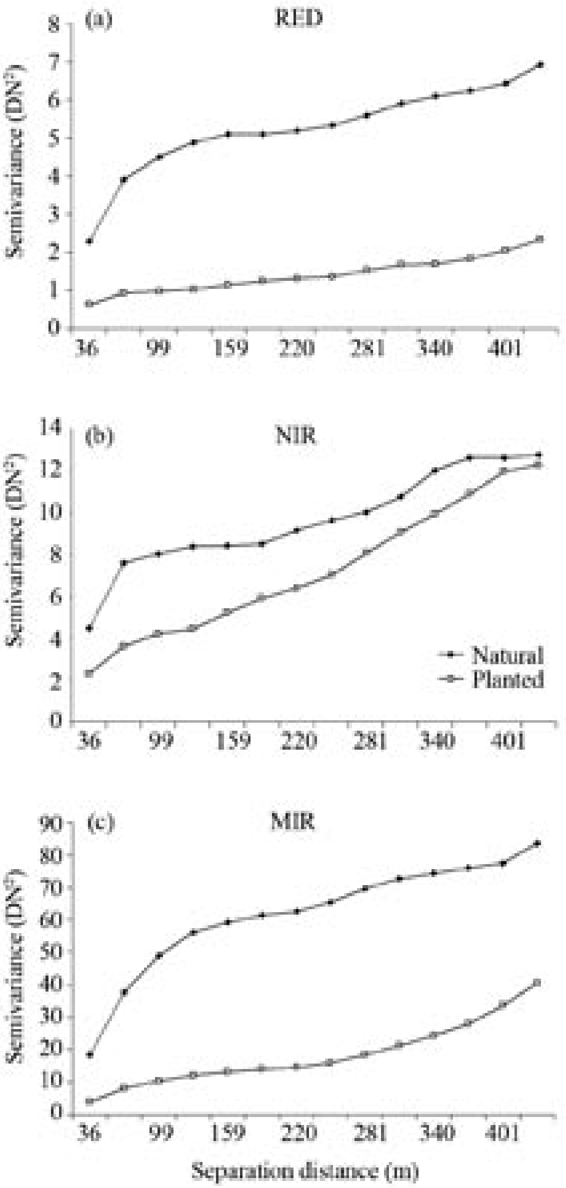

Fig. 3. The exemplary semivariances calculated from (a) RED, (b) NIR, and (c) MIR bands of the remote images of 1,000 m × 1,000 m natural and planted loblolly pine stands

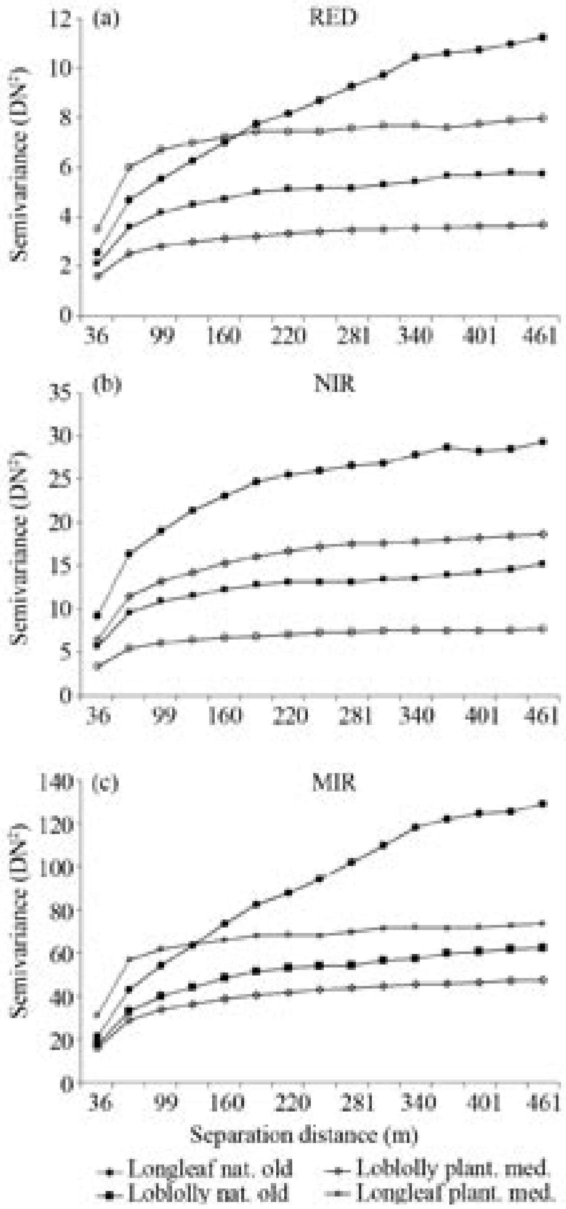

Fig. 4. The semivariances calculated from the remote images of medium and old loblolly pine and longleaf pine stands for the (a) RED, (b) NIR, and (c) MIR bands; lines for natural old longleaf pine in figures (a) and (c) were scaled down by multiplying semivariances by 0.5

semivariances for RED, MIR and NIR bands as well as semivariances for NDVI and RVI indices.

The semivariances were computed in possibly homogeneous and large stands, changing for comparison purposes only one essential stand feature, e.g. age (young, medium, old) or type (planted, natural). The detailed stand parameters are shown in Table 1. The calculations were performed using all possible pairs of pixels in remotely sensed images of investigated stands, for lags changing from about 30 m (the spatial resolution of Landsat TM) with a step of about 30 m, up to about 500 m (approximately half of the length of the smallest forest stand used for the semivariance calculations). The calculations did not show noticeable dependence of semivariances with the change of direction of vector **h**. Therefore in our analyses we concentrated on isotropic (omnidirectional) semivariance for which the direction of separation vector **h** is unimportant. The mean semivariance was then calculated by averaging all semivariances γ_i for the same stand type.

Another measure of spatial correlation analysed in this paper is the cross-semivariance:

$$\gamma_{WZ} = \frac{1}{2N}\sum_{i=1}^{N}[W(x_i) - W(x_i + \mathbf{h})]\,[Z(x_i) - Z(x_i + \mathbf{h})] \quad (2)$$

Table 3. Parameters of semivariogram models fitted to mean experimental semivariograms calculated from investigated stands: nugget (c_0), structural variability connected with exponential model (c_1), range of exponential model (a_1), slope of linear model (c_2), indicative goodness of fit (IGF)

		Loblolly pine					Longleaf pine	
		planted		natural			planted	natural
		young	medium	young	medium	old	medium	old
RED	c_0	0.000	0.000	0.000	0.000	0.000	0.000	0.000
	c_1	6.320	3.188	8.000	5.954	4.231	7.145	22.841
	a_1	128.800	160.070	105.083	252.170	212.84	164.500	344.400
	c_2	0.002	0.001	0.001	0.006	0.002	0.002	0.010
	IGF	1.18E-04	1.15E-04	2.17E-02	4.56E-04	9.56E-04	5.13E-05	4.19E-03
NIR	c_0	0.000	0.000	0.000	0.000	0.000	0.000	0.000
	c_1	15.026	16.036	11.428	17.178	12.368	6.677	60.923
	a_1	191.838	223.153	112.684	243.589	206.692	143.530	128.340
	c_2	0.002	0.006	0.039	0.004	0.004	0.002	0.010
	IGF	4.05E-04	2.06E-04	5.94E-03	3.35E-03	3.31E-03	2.55E-05	1.46E-03
MIR	c_0	0.000	0.000	0.000	0.000	0.000	0.000	0.000
	c_1	72.120	46.040	114.207	77.558	48.227	67.9233	131.229
	a_1	187.906	222.043	98.367	278.160	218.42	128.34	349.96
	c_2	0.009	0.006	0.000	0.083	0.045	0.010	0.159
	Power	1.000	1.000	0.000	1.000	1.000	1.000	1.000
	IGF	1.02E-04	2.42E-04	3.20E-03	2.00E-03	2.28E-03	1.46E-03	1.02E-03
NDVI	c_0	0.000	0.000	0.000	0.000	0.000	×	×
	c_1	0.00425	0.005	0.004	0.006	0.0045	×	×
	a_1	141.55	135.640	122.200	146.300	180.760	×	×
	c_2	1.80E-06	2.70E-06	3.45E-06	2.70E-06	5.00E-07	×	×
	IGF	4.32E-05	5.27E-05	2.62E-04	9.38E-05	9.18E-04	×	×
RVI (NIR/RED)	c_0	0.000	0.000	0.000	0.000	0.000	×	×
	c_1	0.059	0.059	0.059	0.064	0.047	×	×
	a_1	135.289	163.907	108.459	148.557	117.495	×	×
	c_2	1.50E-05	1.80E-05	0.000	8.21E-05	5.40E-05	×	×
	IGF	1.46E-04	8.55E-05	2.51E-04	1.17E-03	7.45E-04	×	×

where: x_i – a data location,
h – a lag vector,
$Z(x_i)$, $W(x_i)$ – the DN values at location x for different bands,
N – the number of data pairs spaced in a distance and direction **h** units apart.

The cross-semivariance quantifies the joint spatial variability (cross-correlation) between two radiometric bands (Deutch, Journel 1998; Jakomulska, Clarke 2001). The experimental cross-semivariances were calculated in the same way as semivariances described above. The obtained experimental semivariances (or cross-semivariances) were used to fit an appropriate theoretical model (McBratney, Webster 1986). These models could allow us to calculate semivariance values that are necessary for other geostatistical analyses such as kriging, cokriging, etc.

All remotely sensed images were analysed using ERDAS 8.5 software. Semivariance calculations and analyses were performed using GS+, version 3.1 (Robertson 1998) as well as Variowin, version 2.2 (Pannatier 1996) geostatistical packages.

RESULTS

The basic descriptive statistics for the remotely sensed images of the studied stands are presented in Table 2. These statistics reveal some distinctions between different stands, but do not provide any textural information. To explore the textural continuity of the studied stands, we calculated and analysed

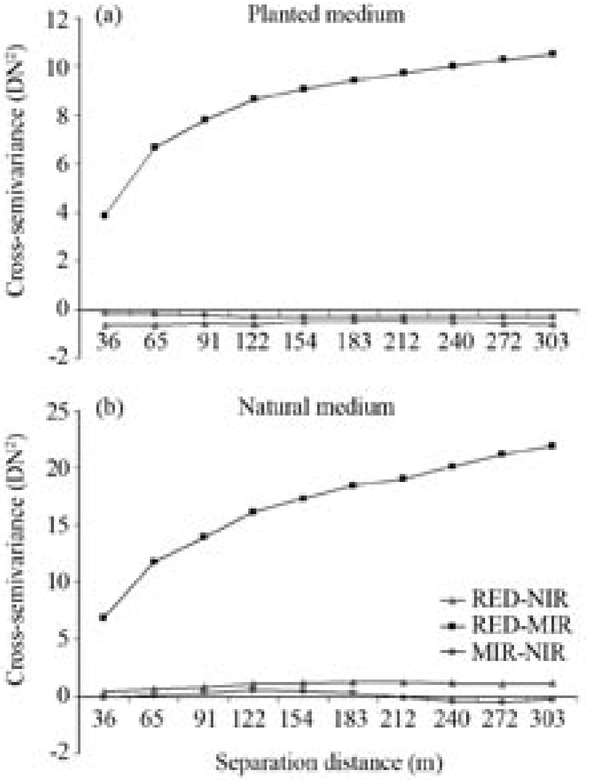

Fig. 5. The cross-semivariances between RED, MIR and NIR bands for (a) planted and (b) natural medium-aged stands of loblolly pine

the semivariances from digital images for RED, MIR and NIR bands as well as the cross-semivariances between these bands. We also calculated the semivariances for the vegetation indices (NDVI and RVI). Fig. 1 shows the most typical shape of semivariograms calculated from Landsat 5 TM images of the investigated stands. The semivariances in this figure were standardised (divided by their variances) in order to show them together. For the small separation distances (a few lags) the semivariance curve rises relatively fast. Then, at the larger distances, it exhibits a gentle sloping and becomes almost linear.

The results of semivariance calculations using DN from RED, NIR and MIR bands as well as the analysed vegetation indices are presented in Fig. 2. The largest differences between semivariances calculated for the investigated loblolly pine stands were obtained from the RED (Fig. 2a) and MIR (Fig. 2c) bands. Distinctly smaller differences were observed between semivariances calculated for DN from the NIR band as well as between semivariances calculated from vegetation indices. Careful examination of Fig. 2 also shows that natural stands have higher semivariance values than equal-age planted stands.

Typical situations in which semivariances were calculated from the images of middle-aged loblolly pine stands of 1,000 m × 1,000 m are shown in Fig. 3. For all bands the semivariances calculated from smaller areas are less regular, but semivariance values for natural stands are still significantly higher than for planted ones. Similarly, as for mean semivariances calculated from all stands of a given type, the largest difference between semivariances was found for the RED and MIR bands (Figs. 3a and 3c).

We also compared semivariograms for different species of pine by calculating semivariances for planted and natural stands of longleaf pine. The corresponding semivariances of loblolly pine and longleaf pine calculated from the DN for the RED, NIR and MIR bands are shown in Fig. 4 (note that the lines for natural old longleaf pine in figures (a) and (c) were scaled down by multiplying semivariances by 0.5). Large differences exist between semivariances calculated from loblolly pine and longleaf pine

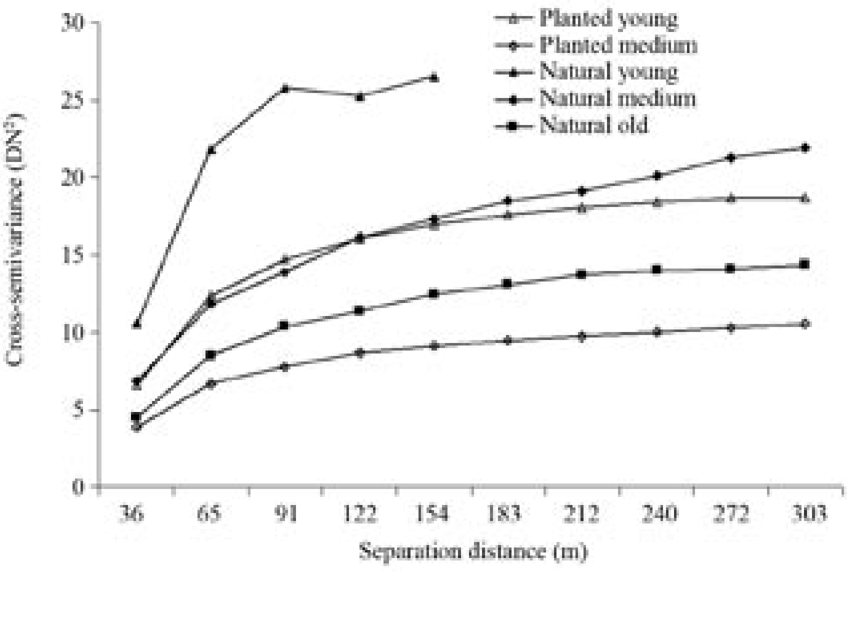

Fig. 6. The cross-correlations between the RED and MIR bands calculated for various loblolly pine stands

stands. Except for the NIR band (Fig. 4b) the values of semivariance for longleaf pine are much higher than those of loblolly pine calculated for the stands of similar type and age. The values of semivariances at the distance of a few lags can also be used as a discriminative parameter.

To check if the parameters of the semivariance model can be used as discriminative parameters for different pine stands, we modelled the above-described experimental semivariances. The best fit of mean experimental semivariances for most of the investigated stands was provided by the sum of the nugget effect model, exponential model and linear model:

$$\gamma_m(\mathbf{h}) = c_0 + c_1\{1 - \exp(-3h / a_1)\} + c_2\mathbf{h} \quad (3)$$

where: c_0 – the nugget value,

c_1 – the structured variability connected with the exponential model,

a_1 – the practical range of the exponential model,

c_2 – the slope of the linear model.

In a few cases for young loblolly pine stands only the nugget effect model and exponential model were used for experimental semivariogram modelling. The parameters of the model semivariances for investigated loblolly pine stands as well as for longleaf pine stands are summarised in Table 3. The Indicative Goodness of Fit (IGF) values for the analysed cases are also shown in Table 3. IGF gives a measure of how well the model of semivariance fits the experimental semivariance points (Pannatier 1996).

Fig. 5 shows the cross-semivariances quantifying the joint spatial variability between two bands calculated between bands RED, MIR and NIR, for planted and natural, medium-aged stands of loblolly pine. The largest cross-correlations exist between the RED and MIR bands both for the planted and for natural stands. The cross-correlations between bands RED and NIR as well as between MIR and NIR are substantially smaller. In the case of natural stands, values of cross-semivariance are much higher than for planted stands (Fig. 5b).

Fig. 6 presents the cross-correlations between the RED and MIR bands calculated for the studied loblolly pine stands. We can see from this figure that all age classes are well separated. The largest cross-semivariance values were obtained for young stands and the smallest for old stands, both for planted and natural ones. Because of the higher semivariance values for natural stands, the semivariances of natural medium and young planted stands are very close to each other.

DISCUSSION

The initial increase of the semivariance curve (Fig. 1) results from the fast decrease of spatial correlation at the distances of a few lags. This means that the spatial correlations between pixels decrease rapidly for short distances. At longer distances the semivariances do not reach saturation but increase almost linearly. This can be explained by a trend that exists in the data. The trend is rather difficult to interpret; it may be caused by many reasons such as for example differential illumination of the imaged area.

In order to check whether the semivariograms can be treated as "spatial signatures" of different types of coniferous forests we calculated semivariances for different types of loblolly pine stands using the DN values from RED, NIR and MIR bands as well as the analysed vegetation indices (NDVI and RVI). Natural stands have higher semivariance values than even-age planted stands (Fig. 2). This can be explained by the higher variability of natural stand textures in comparison with those of planted stands. This tendency was also clearly observed for semivariances calculated from smaller, separate stands (Fig. 3). Distinctly smaller differences were observed between semivariances calculated from vegetation indices (Figs. 2d and 2e). This somewhat surprising behaviour of semivariances calculated using vegetation indices could be explained by the smoothing effect in that these indices are the ratios of DN coming from different bands.

As can be seen in Table 2, the nugget effect is negligible for almost all experimental semivariances under study. The positive slope of the linear model, which describes the trend in the data, is usually very slight. This linear behaviour of the semivariances is distinctly visible only at distances longer than the range of the exponential model. The increase of semivariance caused by the trend at the distance of the range of the exponential model is much smaller than the practical sill of this model. Therefore, the existence of the trend does not interfere with the application of the semivariances for classification of forests using the Landsat 5 TM images.

The most important component in the model of the mean semivariogram $\gamma_m(\mathbf{h})$ is the exponential term with well-defined ranges and sills. Because of the relatively low spatial resolution of the Landsat 5 TM data (30 m), and therefore the large size of support (Jupp et al. 1988, 1989), the ranges within a single stand, connected with the individual trees, are too short to observe. However, a distinct spatial correlation reflected by the exponential model exists at distances many times longer than the Landsat 5 TM spatial resolution (Table 3). The image's spatial properties result from a complex combination of both cover and object size. The correlation described by the exponential model may be attributed to the similarity in arrangements of bigger objects such as small sub-stands or groups of trees, areas with similar understorey, etc. The differences in arrangements of such bigger objects can be dependent on the age and stand origin. Because of the scale of observation, it is not surprising that there is little differentiation between pine stands observed in ranges of the exponential model. However, in spite of the low resolution of the Landsat 5 TM images of pine stands, we found distinct differences in semivariance sills arising from the exponential model (Table 3). The differences depend both on the age and the stand origin. As was shown by Song and Woodcock (2002), at low spatial resolution the semivariance from the scene with larger objects should have a higher sill. One can conclude that the parameters of the exponential term in the semivariance model, especially the sills, quantify well the investigated pine stands and confirm the spatial character of the patterns of forest stands.

The cross-semivariances quantify the joint spatial variability between two bands. The cross-correlations exist between the RED and MIR bands both for the planted and for natural stands as well as much higher values of cross-semivariance for natural stands (Fig. 5). Also, the cross-correlations between the RED and MIR bands are well separated for all analysed age classes (Fig. 6). Therefore, the cross-semivariances, which add new spatial information, can also be used for texture-based classification.

CONCLUSIONS

In the presented study, using semivariances and cross-semivariances, we analyse the spatial properties of low-resolution remote images of loblolly pine and longleaf pine forests of different ages and origins. The semivariances and cross-semivariances were calculated from remotely sensed images of studied stands using digital numbers (DN) and vegetation indices (NDVI and RVI) as data values $Z(x_i)$. The mean semivariances were then calculated by averaging all semivariances for the same stand type (Eq. 2).

The typical mean semivariance shows a relatively fast rise for the few first lags. Then it exhibits a gentle sloping and becomes almost linearly shaped for the larger distances. The small linear increase of semivariances at longer distances can be explained by a trend that may exist in the data. The shapes of semivariances are similar for both very large stands of tens of hectares and small ones of a few hectares. We found distinct differences in mean semivariances of images for the studied stands. This means that in spite of the low-resolution of Landsat 5 TM remote images and the existence of a small trend in the data, the obtained experimental semivariances can be treated as "spatial signatures" for the studied stands.

The observed differences between semivariances at the distances of several lags arise from different spatial correlations existing in the studied stands at distances from a few tens to a few hundreds of meters. A relatively low-resolution of Landsat 5 TM remote images does not allow us to distinguish individual trees. The observed spatial correlations can be attributed to the similarity in arrangements of bigger objects such as groups of trees or small sub-stands, areas with similar understorey, etc. The largest differences in semivariances were obtained for RED and MIR bands. In the cases of these bands the semivariance values for natural stands were remarkably higher than for planted stands. This can be explained by the higher variability of the texture of natural stands in comparison with that of planted stands. The semivariances calculated from vegetation indices for different loblolly pine stands showed much smaller differences than those calculated from the DN of studied bands. This fact can be explained by the smoothing effect arising from the use of DN coming from different bands in vegetation indices and having different spatial properties. It was also evident that the semivariances calculated from Landsat 5 TM images were useful for discriminating different-age loblolly pine stands. We also found large differences between semivariances calculated from images of loblolly pine and longleaf pine stands.

The best fit of mean experimental semivariances for most of the investigated stands was provided by the sum of the three models: the nugget effect model, exponential model, and linear model. It was found that most important in the model of mean semivariance is the exponential term with well-defined range and sill. Both the nugget effect and the contribution to the semivariance arising from a linear term at short distances were significantly smaller than the exponential term. The parameters of the exponential term in the semivariance model, especially the sills, differentiate well the investigated pine stands and confirm the spatial character of the patterns of forest stands.

The cross-semivariances between investigated bands were also calculated and analysed. The largest cross-correlations were found between the RED and NIR bands both for planted and natural loblolly pine stands. The cross-correlations between bands RED and MIR as well as between MIR and NIR were substantially smaller. In the case of natural stands the values of cross-semivariances were much higher than those for planted stands. It was also shown using cross-semivariances that all different-age loblolly pine stands were well separated. The largest cross-semivariance values were obtained for young stands and the smallest ones for old stands, both for planted and natural stands.

This study demonstrates that geostatistical techniques used with relatively inexpensive low-resolution Landsat 5 TM images can be helpful in evaluating spatial characteristics of loblolly pine and longleaf pine stands. High-resolution or multi-resolution satellite investigations, which give the highest accuracy, are still very expensive when they are used over large areas. Therefore, efforts to exploit spatial information from Landsat TM remote images of forest areas are still necessary.

Acknowledgements

Jarosław Zawadzki and Michał Zasada thank the Warnell School of Forest Resources, University of Georgia, for a hospitable and creative environment, Ingvar Elle for help with the English language usage, and Tripp Lowe for technical assistance.

References

ADEGBIDI H.G., JOKELA E.J., COMERFORD N.B., BARROS N.F., 2002. Biomass development for intensively managed loblolly pine plantations growing on spodosols in the southeastern USA. Forest Ecology and Management, *167*: 91–102.

BAUER M.E., BURK T.E., EK A.R., COPPIN P.R., LIME S.D., WALSH T.A., WALTERS D.K., BEFORT W., HEIZEN D.F., 1994. Satellite Inventory of Minnesota Forest Resources. Photogrammetric Engineering & Remote Sensing, *60*: 287–298.

BROCKHAUS J.A., KHORRAM S., 1992. A comparison of SPOT and Landsat-TM data for use in concluding inventories of forest resources. International Journal of Remote Sensing, *13*: 3035–3043.

BROWN L., CHEN J.M., LEBLANC S.G., CHILLAR J., 2000. A short-wave infrared modification to the simple ratio for LAI retrieval in boreal forests: an image and model analysis. Remote Sensing of Environment, *71*: 16–25.

CAMPBELL J.B., 1994. Introduction to Remote Sensing. New York, Guilford Press: 1–20.

CARR J.R., 1966. Spectral and textural classification of single and multiple band digital images. Computers & Geosciences, *22*: 849–866.

CHICA-OLMO M., ABARCA-HERNANDEZ F., 2000. Computing geostatistical image texture for remotely sensed data classification. Computers & Geosciences, *26*: 373–383.

COHEN W.B., SPIES T.A., BRADSHAW G.A., 1990. Semivariograms of digital imagery for analysis of conifer canopy structure. Remote Sensing of Environment, *34*: 167–178.

CURRAN P.J., 1988. The semivariances in remote sensing: an introduction. Remote Sensing of Environment, *24*: 493–507.

DE FRIES R.S., TOWNSHEND J.R.G., 1994. NDVI-derived land cover classifications at a global scale. International Journal of Remote Sensing, *15*: 3567–3586.

DE JONG S.M., 1994. Derivation of vegetative variables from a Landsat TM image for modelling soil erosion. Earth Surfaces and Landforms, *19*: 165–178.

DEUTCH C.V., JOURNEL A.G., 1998. GSLIB Geostatistical Software Library. Oxford, Oxford University Press: 43–62.

ERDAS Field Guide, 1990. Fifth Edition. Atlanta, Georgia, Erdas Inc.: 101–106.

EVANS D.L., 1994. Forest Cover from Landsat Thematic Mapper Data for Use in the Catahoula Ranger District Geographic Information System. Gen. Tech. Rep. SO-99. New Orleans, LA: U.S. Department of Agriculture, Forest Service, Southern Forest Experiment Station: 14.

HARMS W.R., 1984. Applying silviculture to stand management. In: KARR B.L., MONAGHAN T. (eds.), The Loblolly Pine Ecosystem (West Region) Proceedings, March 20–22, Jackson, MS. Mis. Coop. Extension Serv., Mississippi State, MS: 32–40.

HERZFELD U.C., HIGGINSON C.A., 1996. Automated geostatistical seafloor classification – principles, feature vectors, and discrimination criteria. Computers & Geosciences, *22*: 35–52.

JAKOMULSKA A., CLARKE K., 2001. Semivariogram-derived measures of textural image classification. In: MONESTIEZ P., ALLARD D., FROIDEVAUX R. (eds.), Geostatistics for Environmental Applications. Dordrecht Hardbound, Kluwer Academic Publishers: 345–355.

JORDAN C.F., 1969. Derivation of leaf area index from quality of light on the forest floor. Ecology, *50*: 663–666.

JOURNEL A.G., HUIBREGTS C.J., 1978. Mining Geostatistics. London, Academic Press: 26–95.

JUPP D.L.B., STRAHLER A.H., WOODCOCK C.E., 1988. Autocorrelation and regularization in digital images. I. Basic theory, IEEE Geosciences and Remote Sensing, *26*: 467–473.

JUPP D.L.B., STRAHLER A.H., WOODCOCK C.E., 1989. Autocorrelation and regularization in digital images. I. Simple image models. IEEE Geosciences and Remote Sensing, *27*: 247–258.

McBRATNEY A.B., WEBSTER R., 1986. Choosing function for semivariograms of soil properties and fitting them to sampling estimates. Journal of Soil Sciences, *37*: 617–639.

MIRANDA F., MAcDONALD J., CARR J.R., 1992. Application of the semivariogram textural classifier (STC) for vegetation discrimination using SIR-B data of Borneo. International

Journal of Remote Sensing, *13*: 2349–2354.
MIRANDA F., FONESCA L., CARR J.R., TARANIK J., 1996. Analysis of JERS-1 (Fuyo-1) SAR data for vegetation discrimination in northwestern Brazil using the semivariogram textural classifier (STC). International Journal of Remote Sensing, *17*: 3523–3529.
NEMANI R., PIERCE L., RUNNING S., 1993. Forest ecosystem process at the watershed scale: Sensitivity to remotely-sensed Leaf Area Index estimates. International Journal of Remote Sensing, *14*: 2519–2539.
PANNATIER Y., 1996. Variowin, Software for Spatial Data Analysis in 2D. New York, Berlin, Heidelberg, Springer-Verlag: 1–91.
RAMSTEIN G., RAFFY M., 1989. Analysis of the structure of radiometric remotely-sensed images. International Journal of Remote Sensing, *17*: 3523–3529.
ROBERTSON G.P., 1998. GS+ user's guide: geostatistics for the environmental sciences, version 3.1 for Windows. Gamma Design Software, Plainwell, MI.
ROUSE J.W., HAAS R.H., SCHELL J.A., DEERING D.W., 1973. Monitoring vegetation systems in the great plains with ERTS. In: Proceedings, Third ERTS Symposium, NASA SP-351, NASA, Washington, DC, *1*: 309–317.
SHEFFIELD R.M., KNIGHTS H.A., 1982. Loblolly pine resources – South-east region. In: Proceedings, Symposium on the Loblolly Pine Ecosystem (East Region). School of Forest Resources, North Carolina State University, Raleigh, NC: 7–24.
SONG C., WOODCOCK C.E., 2002. The spatial manifestation of forest succession in optical imagery. The potential of multiresolution imagery. Remote Sensing of Environment, *82*: 271–284.
STRAHLER A.H., WOODCOCK C.E., SMITH J.A., 1986. On the nature of models in remote sensing. Remote Sensing of Environment, *20*: 121–139.
ST-ONGE B.A., CAVAYAS F., 1995. Estimating forest stand structure from high resolution imagery using the directional semivariogram. International Journal of Remote Sensing, *16*: 1999–2001.
TUCKER C.J., FUNG I.Y., KEELING C.D., GAMMON R.H., 1986. Relationship between atmospheric CO_2 variations and a satellite-derived vegetation index. Nature, *319*: 195–199.
TREITZ P., HOWARTH P., 2000. High spatial remote sensing data for forest ecosystem classification: an examination of spatial scale. Remote Sensing of Environment, *72*: 268–289.
VOGELMANN J.E., SOHL T.L., CAMPELL P.V., SHAW D.M., 1998. Regional land cover characterization using Landsat Thematic Mapper data and ancillary data sources. Environmental Monitoring and Assessment, *51*: 415–428.
WALLACE C.S.A., WATTS J.M., YOOL S.R., 2000. Characterizing the spatial structure of vegetation communities in the Mojave Desert using geostatistical techniques. Computers & Geostatistics, *26*: 397–410.
WOODCOCK C.E., STRAHLER A.H., JUPP D.L.B., 1988a. The use of semivariograms in remote sensing: I. Scene models and simulated images. Remote Sensing of Environment, *25*: 323–348.
WOODCOCK C.E., STRAHLER A.H., JUPP D.L.B., 1988b. The use of semivariograms in remote sensing: II. Real digital images. Remote Sensing of Environment, *25*: 349–379.

Received for publication October 20, 2004
Accepted after corrections November 29, 2004

Semivariogramová analýza textury dat z Landsatu TM 5 u porostů borovice kadidlové (*Pinus taeda* L.)

J. Zawadzki[1], Ch. J. Cieszewski[2], M. Zasada[3]

[1]*Environmental Engineering Department, Warsaw University of Technology, Warsaw, Poland*
[2]*Warnell Scholl of Forest Resources, University of Georgia, Athens, USA*
[3]*Department of Forest Productivity, Faculty of Forestry, Warsaw Agricultural University, Warsaw, Poland*

ABSTRAKT: Cílem studie bylo zhodnotit použitelnost snímků z družice borových porostů v západní Georgii ve Spojených státech. Při analýze prostorových korelací mezi pixely měřenými pomocí semivariancí a křížových semivariancí (křížové korelace mezi dvěma radiometrickými pásmy), počítanými z transektů ve snímcích z družice Landsat TM, jsme zjistili rozdíly mezi semivariancemi vztahujícími se ke snímkům porostů různého stáří, původu (přirozené versus uměle založené porosty) a druhu (borovice kadidlová *Pinus taeda* L. versus borovice bahenní *Pinus palustris* Mill.). Analyzovali jsme jak pozemní měření, tak družicové snímky využívající viditelné, blízké infračervené a střední infračervené pásmo spektra. Také jsme analyzovali semivariance a křížové semivariance vypočtené z normalizovaného diferenčního indexu vegetačního pokryvu (Normalized Difference Vegetation Index) a vegetačního indexu (Ratio Vegetation Index). Výsledky ukázaly, že přes relativně malé prostorové rozlišení Landsatu TM semivariogramy a křížové semivariogramy poskytly potenciálně užitečnou informaci o uvedených třídách. Semivariance a křížové semivariance počítané na snímku Landsatu TM pro borovici kadidlovou a borovici bahenní závisejí jak na věku, tak na původu porostu. Velké rozdíly existují zejména v prazích semivariancí a křížových semivariancí. Významné diference existují také mezi semivariancemi počítanými z porostů borovice kadidlové a bahenní.

Klíčová slova: semivariance; klasifikace textury; dálkový průzkum Země; borovice kadidlová; satelit Landsat TM

Corresponding author:

Dr. inž. Jaroslaw Zawadzki, Environmental Engineering Department, Warsaw University of Technology, Nowowiejska 20, 00-653 Warsaw, Poland
tel.: + 48 22 660 5426, fax: + 48 22 625 4305, e-mail: jaroslaw.zawadzki@is.pw.edu.pl